



Article citation info:

Hryciów Z, Rybak P, Wojciechowski M, Wachowiak P, Kalicki B, Hydropneumatic suspension testing of a wheeled armoured personnel carrier *Eksploracja i Niezawodność – Maintenance and Reliability* 2023; 25 (2) <http://doi.org/10.17531/ein/162497>

## Hydropneumatic suspension testing of a wheeled armoured personnel carrier

Indexed by:



Zdzisław Hryciów<sup>a,\*</sup>, Piotr Rybak<sup>a</sup>, Michał Wojciechowski<sup>b</sup>, Przemysław Wachowiak<sup>b</sup>, Bartosz Kalicki<sup>c</sup>

<sup>a</sup> Instytut Pojazdów i Transportu, Wojskowa Akademia Techniczna, Poland

<sup>b</sup> Laboratorium Badań Pojazdów Gąsienicowych, Military Institute of Armoured and Automotive Technology, Poland

<sup>c</sup> Ministry of National Defence, Poland

### Highlights

- Hydropneumatic (HP) suspension allows easy design of spring characteristic.
- Simulation studies of HP suspension usually assume a polytropic gas process.
- Static deflection decreases with increasing temperature and initial gas pressure.
- Friction in the seals is an important source of resisting force.
- The HP struts heat up considerably during operation of the carriers.

### Abstract

The purpose of this study was to determine the effect of gas pressure and temperature on the spring characteristic of a HP strut used in a wheeled armoured personnel carrier. The research was performed based on a simulation model. Data to validate the model were obtained during experimental tests. The results indicate, among other things, that the friction generated in the seals is an important source of resistance force. Comparison of the simulation results with the measured characteristics indicates a proper modelling of the strut operation. Simulation studies have indicated that it is easy to modify the required suspension parameters by adjusting the initial gas pressure. A linear effect of pressure on static deflection can be assumed. Temperature has a strong influence on the spring characteristic. When it changes, significant changes in vehicle height are observed due to the lack of a compensation system. The temperature changes are not only due to changes in ambient temperature, but also by intense heating of the HP struts caused by the vehicle moving over rough terrain.

### Keywords

hydropneumatic suspension, polytropic process, spring characteristic, static deflection

This is an open access article under the CC BY license (<https://creativecommons.org/licenses/by/4.0/>)

### 1. Introduction

The most common spring elements used in vehicle suspensions can include metal, pneumatic and hydropneumatic (HP) elements. Suspensions based on metal spring elements are the most commonly used due to their simple design and relatively low cost. However, a major limitation of these is the difficulty in designing non-linear spring characteristic. HP suspension have an important advantage. They integrate spring and damping elements in a single system. Unfortunately, their main disadvantage is their high cost. They also have a more complex

design than metal spring elements, and are more complicated and time-consuming to maintain [2]. The basic components of the system are a hydraulic cylinder and a HP accumulator, filled with working fluids.

HP suspension is mainly used where vehicle height adjustment is required [10], where there is limited space to install system components, where there is a need to lock the suspension, and where a change in suspension stiffness is required. For this reason, this type of suspension is often used

(\*) Corresponding author.

E-mail addresses:

Z. Hryciów (ORCID: 0000-0002-6281-1883) [zdzislaw.hryciow@wat.edu.pl](mailto:zdzislaw.hryciow@wat.edu.pl), P. Rybak (ORCID: 0000-0002-7063-9913) [piotr.rybak@wat.edu.pl](mailto:piotr.rybak@wat.edu.pl), M. Wojciechowski (ORCID: 0000-0001-8947-5931) [michal.wojciechowski@witpis.eu](mailto:michal.wojciechowski@witpis.eu), P. Wachowiak (ORCID: 0000-0003-2336-7844) [przemyslaw.wachowiak@witpis.eu](mailto:przemyslaw.wachowiak@witpis.eu), B. Kalicki [s-kalicki@outlook.com](mailto:s-kalicki@outlook.com)

in modern military vehicle designs [2, 12, 15], as well as in the construction of agricultural machinery [18]. It also offers many more possibilities in the development of active suspension. It allows not only the damping force, but also the stiffness characteristic to be adjusted [20].

An important advantage of HP suspension used on multi-axle vehicles is that the ground reaction force for each wheel can be easily adjusted. Similarly, by regulating the initial pressure value, it is possible to hold a constant ground clearance value for the vehicle regardless of its weight. This is particularly useful for multi-axle armoured personnel carriers, on which armament and/or other equipment with different weights is mounted on a common chassis [7].

Models that simulate the operation of a HP strut are an important tool in the correct design of vehicle's suspension. In the literature, works related to the modelling of HP suspension [3, 9, 12] concern the study of their individual components as well as cover issues related to the modelling of vehicle dynamics [4, 16, 19]. However, due to the variety of designs, they cannot always be generalised to other solutions.

An important issue in HP suspension modelling is the correct representation of the gas compression/expansion process, and hence obtaining the correct relationship between suspension deflection and spring force. In most HP suspension systems, nitrogen ( $N_2$ ) is used as the working gas. This is mainly due to the availability and inertness of the gas.

In the modelling process, the most common approach is to use a perfect gas model and the compression of the gas is described by a polytropic process. Depending on the polytropic exponent  $n$ , it takes values between isothermal ( $n = 1$ ) and adiabatic ( $n = k$ ). The value of  $k$  for nitrogen (an ideal gas) is 1.4 at 300 K. Due to the frequencies of the suspension (usually ranging from 1 to several Hz), the changes of state of the gas (its pressure, volume and temperature) are so quick that only a small part of the heat is dissipated [2, 11] and the gas process is therefore close to an adiabatic one. It is not possible to determine the exact amount of heat dissipated and therefore the exact value of the polytropic exponent. It varies continuously during the operation of the suspension. Therefore, in many papers, its value is arbitrarily assumed as the most appropriate representation of the operation of the suspension. This value is usually in the range 1.3 - 1.35 [2, 5, 14].

The use of the real gas equation is less common. The paper [18], analysed the usefulness of complex gas process models. The implementation of the BWR (Benedict Webb Rubin) model was found to best represent the gas process in HP suspension. At low forcing frequencies, good agreement is also obtained with the assumption of an isothermal process, while at higher frequencies the assumption of an adiabatic process is obtained.

In operation, vibration damping is provided by viscous damping and friction at sliding interfaces. The frictional force is mainly generated in sealing systems. It should be noted that its value varies significantly with system pressure and load [1, 11, 13]. The Stribeck and LuGre models are most commonly used to describe friction in hydraulic cylinder seals [14, 17].

In a HP strut, as in hydraulic shock absorbers, the vibration energy is dissipated as heat [19]. At high vibration amplitudes and poor heat transfer, this leads to heating of the hydraulic oil and changes in its damping properties [6, 8]. In addition, the volume of oil and gas also increases and so does the deflection of the HP strut. In multi-axle vehicles, this can lead to a change in the distribution of wheel load forces on the following axles.

It is noticeable, that in the available literature, there is a lack of work related to the above mentioned issues, particularly the effect of temperature. In military vehicles, efforts are made to keep the design as simple as possible, to increase reliability and to reduce control systems to the minimum necessary, however, it should be emphasized that changes in operating conditions (mainly temperature and initial system gas pressure) can significantly affect the value of the vehicle ground clearance and the load on its wheels. Therefore, the main objective of this study was to determine the effects of initial system pressure and temperature on the spring characteristic and static deflection values of a HP strut mounted in a carrier. The study was based on a developed and validated model of a HP strut used in a wheeled armoured personnel carrier. The acquisition of data for model validation required the determination of basic spring and damping characteristics. An additional aim of the study was to estimate the way in which the HP struts heat up as the vehicle moves over rough roads and to determine their influence on wheel load and vehicle height change.

## 2. Hydropneumatic strut test methodology

The test object was a HP strut used in a wheeled armoured

personnel carrier. The HP strut was tested using an Instron 8802 universal testing machine capable of both static and dynamic testing. The test programme included the determination of quasi-static characteristics over the full stroke range, as well as the performance of dynamic tests with an amplitude of  $A = 10$  mm, in the frequency range  $f = 0.1 - 1$  Hz. The above parameters are determined by the capabilities of the testing machine. A view of the HP strut mounted in the testing machine is shown in Fig. 1. Prior to testing, the nitrogen pressure in the gas chamber was checked. It was 4.8 MPa. The temperature in the room where the HP strut was stored and the tests were performed was 22°C. The tests were carried out at relatively low movement velocities (up to about 60 mm/s), so that no significant heating of the strut was observed

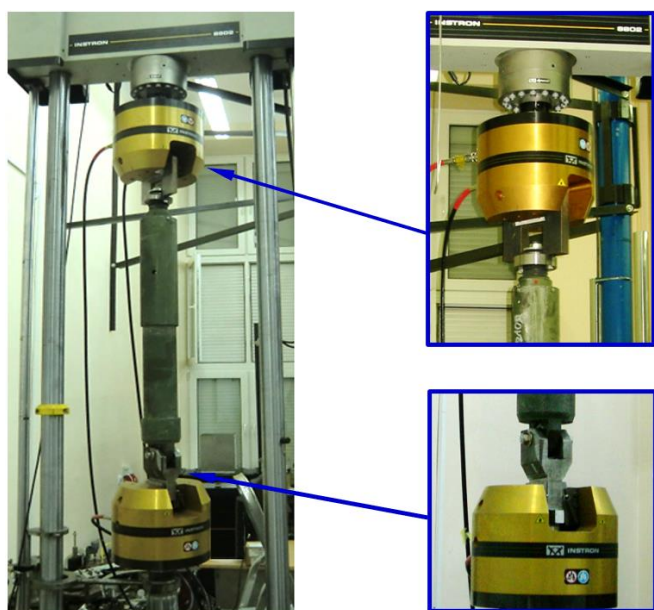


Fig. 1. View of the HP strut mounted in the testing machine.

### 3. Hydropneumatic strut model

A cross-section and schematic diagram of the HP strut is shown in Fig. 2. It indicates, among other things, the forces and pressures acting on selected components and displacements of the strut's elements. The system used on the carrier allows the vehicle's ground clearance to be adjusted only when stationary. During normal operation, the valves connecting the strut to the external system remain closed. Thus, the amount of gas in the chamber remains constant. There are three main chambers inside the strut. The upper chamber, filled with high-pressure nitrogen, is separated from the middle chamber, filled with hydraulic fluid, by a moving piston. The third - lower - chamber is located in the outer cylinder. It is also filled with oil. Between

the oil chambers there is a valve that throttles the flow when the piston and cylinder move relative to each other. This valve acts as a vibration damper. As the strut is compressed, some of the oil from the central chamber additionally flows into the space between the inner and outer cylinder.

In the diagram, the pressures in each chamber are shown as follows: in the gas chamber the pressure is  $p_g$ , in the oil chamber the pressures are  $p_{o1}$  and  $p_{o2}$  respectively.

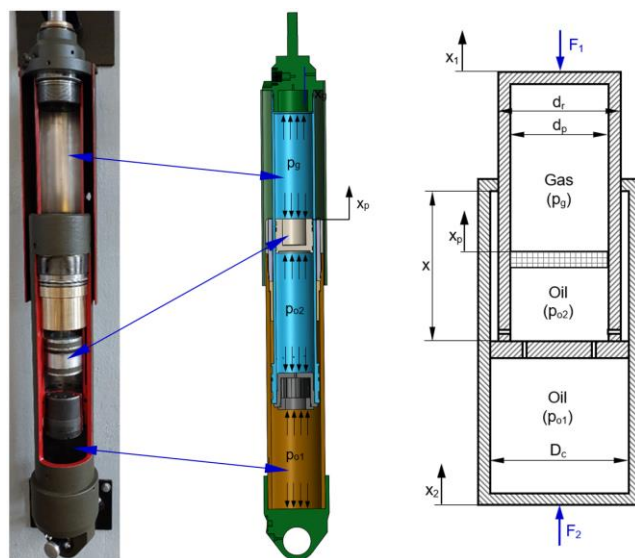


Fig. 2. Cross-section and scheme of hydropneumatic strut design.

Assuming small values for the inertial forces acting on the strut components (relative to the spring force of the gas), it can be assumed that the values of the forces at both ends are equal. The deflection of the strut  $x$  is the difference in displacement between the two ends ( $x_2 - x_1$ ). The pressure changes in the gas section is described by the equation (1):

$$p_g \cdot V_g^n = p_{g,0} \cdot V_{g,0}^n \quad (1)$$

The index 0 indicates the volumes in the initial state (for a maximally stretched strut, i.e.,  $x = 0$ ). Assuming that the oil is incompressible, the sum of the volumes of the oil chambers remains constant (2):

$$V_{o1_0} + V_{o2_0} = V_{o1_0} - x \cdot A_{o1} + V_{o2_0} + x_p \cdot A_{o2} + x \cdot A_d = const \quad (2)$$

where:  $A_{o1}$  and  $A_{o2}$  – the cross-sectional areas of the oil chambers of diameter  $D_c$  and  $d_p$ ,

$x_p$  – displacement of the moving piston,

$A_d$  – cross-sectional area of the additional chamber ( $A_d = 0.25 \cdot \pi \cdot (D_c^2 - d_r^2)$ ).

Hence the displacement of the piston  $x_p$  is (3):

$$x_p = x \frac{(A_{o1} - A_d)}{A_{o2}} \quad (3)$$

Finally, the current value of the gas chamber volume can be calculated using the equation (4):

$$V_g = V_{g0} - x \cdot (A_{o1} - A_d) \quad (4)$$

The spring force can be calculated from the equation (5):

$$F_g = p_g \cdot A_g = p_{g_0} \cdot A_g \cdot \left( \frac{V_{g_0}}{V_{g_0} - x \cdot (A_{o1} - A_d)} \right)^n \quad (5)$$

When the vehicle is moved over rough terrain, intense heating of the HP strut is observed. In the absence of a working fluid volume compensation system, a change in the static deflection of the HP strut is observed. In the model developed, the incompressibility of the oil was assumed, while the volume changes of oil and nitrogen due to their temperature expansion were taken into account. A linear model of volume change with temperature was assumed for the oil (6):

$$V_{o,T} = V_{o,0} \cdot (1 + \beta \cdot \Delta T) \quad (6)$$

where:  $V_{o,0}$  and  $V_{o,T}$  – total volume of oil chambers before and after temperature increase,

$\beta$  – volumetric coefficient of thermal expansion of oil,

$\Delta T$  – temperature increase.

The calculation assumes a coefficient of volumetric thermal expansion  $\beta_o = 0.0008$  1/K. The variation of nitrogen pressure with temperature change is determined by the isochoric process equation (keeping the gas volume constant when the strut is fully extended).

## 4. Test results

### 4.1. The main characteristics of HP strut

The main characteristics of the HP strut were determined using sinusoidal excitation. In the first test step, the displacement

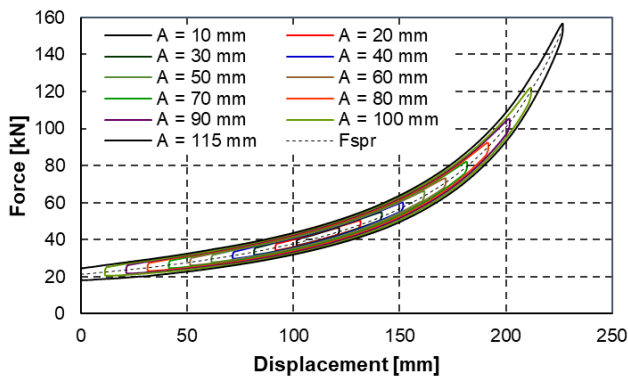


Fig. 3. Force–displacement characteristic.

amplitude was varied from 10 to 100 mm at a constant

excitation frequency of 0.1 Hz. In the final step, measurements were taken for  $A = 115$  mm, where the strut was completely stretched. For each variant, the force and the displacement values were recorded. From the results obtained, the centre line corresponding to the value of the compressive force was determined (Fig. 3).

To determine the variation of resistance forces depending on displacement and velocity, the value of the spring force was subtracted from the recorded loops (Fig. 4).

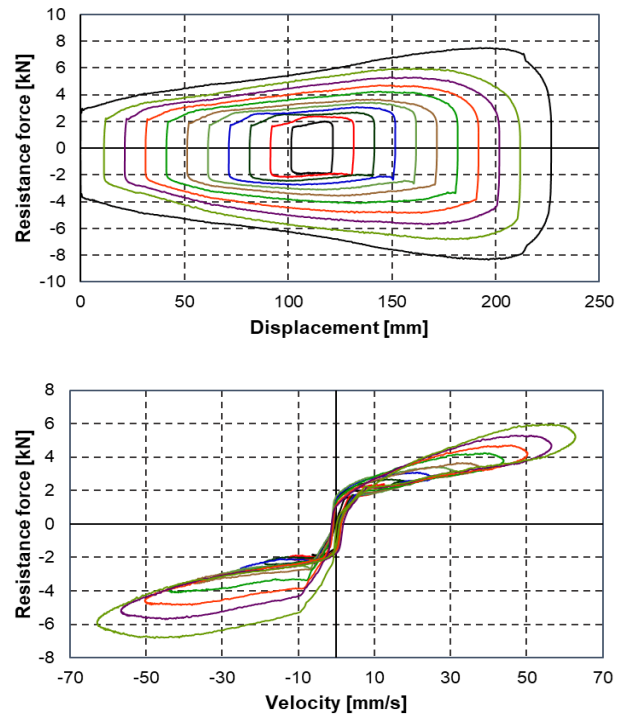


Fig. 4. Variation of resistance force as a function of displacement  $F_r = f(x)$  and velocity  $F_r = f(v)$ .

For a displacement amplitude of 115 mm, the maximum velocity of the piston movement of the testing machine was reached. Hence, the obtained motion velocity waveform deviated from the harmonic function. Therefore, this waveform was not included in the characteristic of the resistance force as a function of velocity. Analysing the obtained results, it can be seen that there is a step change in the resistance force at the points where the direction of movement changes. This is mainly related to the frictional force in the seals. Its value, for smaller values of HP strut compression, is about 2 kN. However, as the strut is compressed (working fluid pressure increases), an increase in the value of the resistance forces is also observed. This is due to the additional pressure of the seal against the cylinder surface.

In order to determine more precisely the impact of velocity on the value of the damping force, tests were carried out with a constant displacement amplitude of 10 mm (Fig. 5). The tests were performed with an initial strut compression of 112 mm - this corresponds approximately to the static deflection value of the strut mounted on the vehicle. The motion frequency was varied from 0.1 to 1 Hz. This increased the velocity of the piston movement at a similar working fluid pressure, and thus succeeded in reducing the effect of the changing friction force on the total resistance forces. For frequencies up to approximately 0.4 Hz (corresponding to a maximum velocity of 25 mm/s), no significant change in resistance forces as a function of velocity is observed. In this velocity range, the frictional force is the dominant source of resistance. With increasing the velocity beyond this range, a significant increase in the viscous damping force is observed. Unfortunately, due to the limited capabilities of the testing machine, it was not possible to determine the damping characteristic for higher movement velocities (also specifying the limit velocity at which the pressure limiting valve opens).

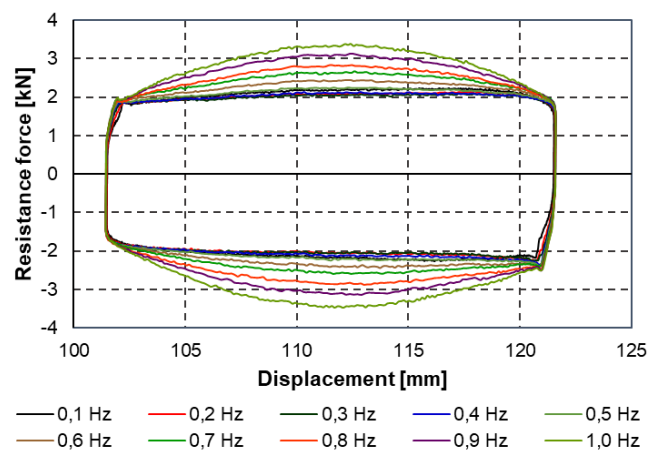
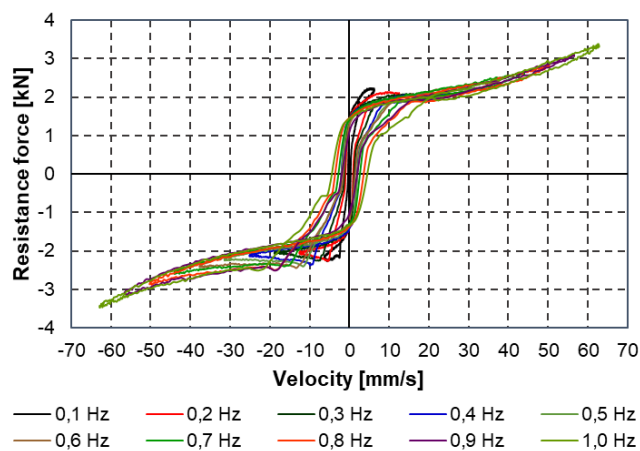


Fig. 6. Changes in resistance force as a function of displacement  $F_r = f(x)$  and velocity  $F_r = f(v)$ .

The dissipated energy value was calculated for each complete cycle based on received changes in resistance force as a function of amplitude and frequency (Table 1). It was determined from the equation:

$$E_c = \oint F dx, \quad (7)$$

From the results obtained, it can be concluded that, in the velocity range considered, the value of the energy dissipated per

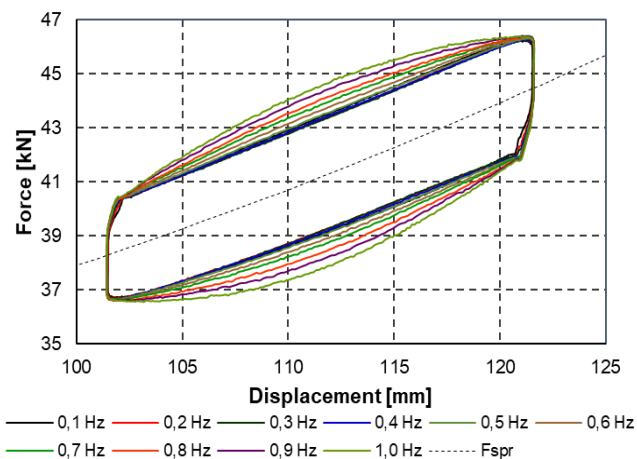


Fig. 5. Characteristics of the HP strut  $F = f(x)$ .

As in the previous case, the value of the spring force was subtracted from the results obtained. This resulted in changes in the resistance force as a function of the displacement and velocity of the HP strut. The average value of the resistance force due to friction is approximately 2 kN (although Fig. 6 shows a slight increase in this force as the strut is compressed). Due to the limitations of the testing machine, the damping characteristic were only determined up to about 60 mm/s.

cycle is approximately proportional to the square of the displacement amplitude. It also depends in a similar way on the frequency. It should be noted that once the limit velocity for which the pressure-limiting valve is opened is exceeded, the value of the resistance force, and thus of the dissipated energy, ceases to increase rapidly.



Table 1. Summary of energy dissipation values.

| Frequency 0.1 Hz |     |     |     |     |     |     |      |      |      |      |
|------------------|-----|-----|-----|-----|-----|-----|------|------|------|------|
| Amplitude [mm]   | 10  | 20  | 30  | 40  | 50  | 60  | 70   | 80   | 90   | 100  |
| Energy [J]       | 80  | 166 | 280 | 414 | 575 | 757 | 1002 | 1290 | 1623 | 2030 |
| Amplitude 10 mm  |     |     |     |     |     |     |      |      |      |      |
| Frequency [Hz]   | 0.1 | 0.2 | 0.3 | 0.4 | 0.5 | 0.6 | 0.7  | 0.8  | 0.9  | 1.0  |
| Energy [J]       | 80  | 80  | 81  | 82  | 85  | 90  | 96   | 101  | 108  | 116  |

#### 4.2. Model validation

Based on the mathematical model, Matlab programme has been created to simulate the operation of a HP strut. It allows the value of the gas spring force to be determined as a function of strut deflection for different values of initial pressure in the gas chamber and initial gas temperature. A polytropic exponent of 1.3 was used in the calculations. Fig. 7 shows the changes in spring force obtained from the calculations compared to the experimental results. The calculations were performed for an initial pressure of 4.8 MPa and an initial temperature of 20°C. Close agreement was obtained between the simulation and the experimental results. In the range of deflections up to about

200 mm, the relative difference is less than 2%. Only for the maximum deflections an increase in the difference is observed - for the maximum deflection the difference is about 10%. In order to improve the quality of the model in this range, it is necessary to consider changes in the polytropic exponent as a function of gas pressure and temperature. The rate of pressure change induced by the compression/extension velocity of the strut must also be taken into account. At low velocities, the gas process will be closer to an isotropic one, while at higher velocities it will be closer to an adiabatic one. It is therefore necessary to adjust the polytropic exponent to the actual test conditions.

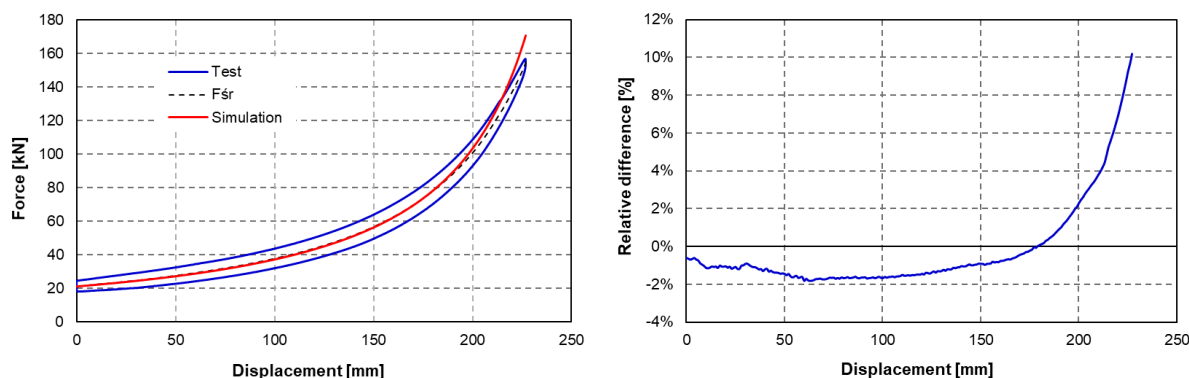


Fig. 7. Spring characteristics of the HP strut  $F = f(x)$  (left) and relative difference of force (right).

#### 4.3. HP strut simulation studies

Based on the developed model, HP strut simulations were carried out. The scope of the studies included:

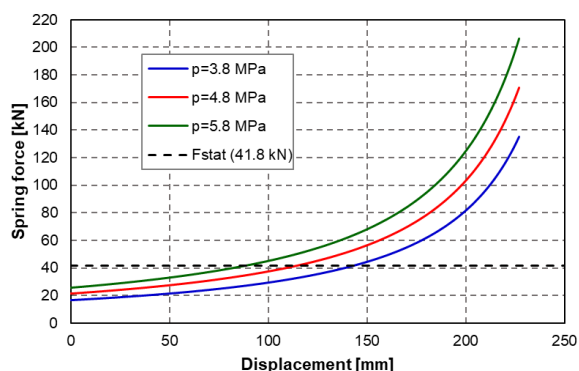
- determination of the influence of the initial pressure in the gas chamber on the spring characteristics; the pressures were varied in the range  $3.8 \div 5.8$  MPa, in 0.2 MPa steps,
- determination of the influence of the initial gas temperature on the spring characteristics; the temperature value was varied in the range of  $-30 \div +80$ °C, in 10°C steps.

The lowest temperature value corresponds to the most common permissible operating conditions for armoured personnel carriers. The static deflection value (at a force of

41.8 kN) was also calculated for each variant, as well as the coefficient of elasticity around this point. The effect of variations in initial pressure was determined at 20°C, while the temperature was determined at an initial pressure of 4.8 MPa.

Fig. 8 shows the variation of the gas spring force as a function of strut compression for three initial pressure values. From the obtained characteristics, it can be seen that a pressure changes of 1 MPa from the nominal value (4.8 MPa) results in a change in the spring force of approximately 20%. The largest differences occur at the maximum compression of the HP strut (approximately 35 kN for a pressure change of 1 MPa from the nominal value). The static deflection value decreases approximately linearly by about 27 mm/MPa for the range of

pressure changes considered. As the pressure increases,



a reduction in stiffness is observed around the static deflection point.

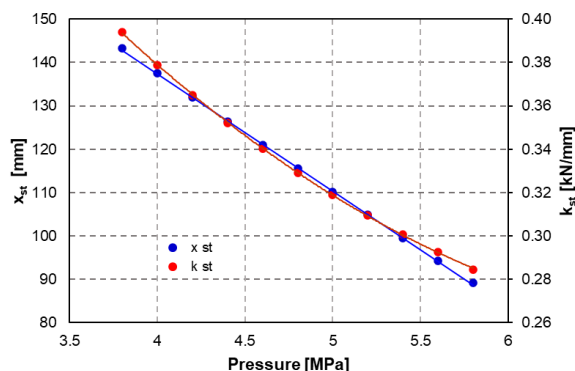


Fig. 8. HP strut characteristics:  $F = f(x)$ ,  $x_{st} = f(p)$  and  $k_{st} = f(p)$ .

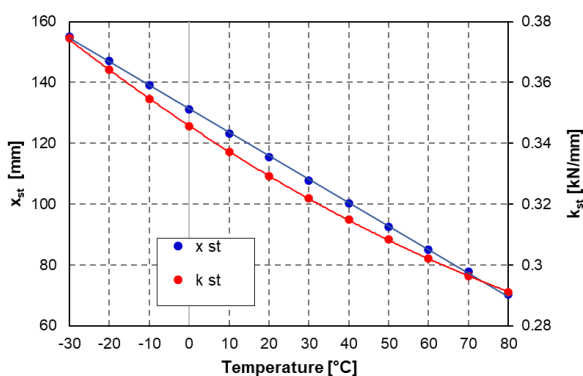
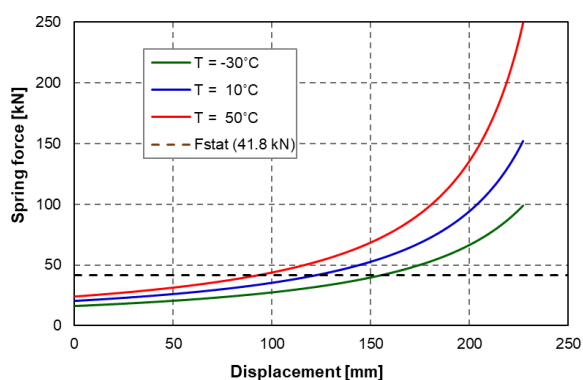


Fig. 9. HP strut characteristics:  $F = f(x)$ ,  $x_{st} = f(T)$  and  $k_{st} = f(T)$ .

Fig. 9 shows the effect of the changing the initial temperature on the static deflection and the spring coefficient around the static equilibrium point. Again, the nature of the change in static deflection is approximately linear. The static deflection decreases by approximately 0.77 mm/°C. For the same initial pressure value in the system, a change in temperature from -20 to 20°C (e.g., winter to summer) will result in a change in the static deflection value of approximately 32 mm. At low temperature, the value of the spring force decreases significantly. In combination with the increased static deflection, this raises the probability that the dynamic stroke of the suspension will be exhausted during off-road driving.

#### 4.4. Testing the effect of temperature on the suspension static deflection

An important component of the HP suspension system is the pressure accumulation system. Without it, the static deflection and stiffness of the suspension will change as a result of increasing or decreasing oil and gas volumes. For multi-axle vehicles, the issue is more complex. There is an uneven heating

of the HP struts of the individual axles. The temperature changes most rapidly on the first axle of the vehicle (due to the highest dynamic deflections). In multi-axle chassis, the static deflections of the individual struts are related to each other. Therefore, a change in temperature leads to a change in the normal reaction forces of the individual wheels. Among other things, this changes the loads acting on the vehicle components, but also on the maximum braking force that can be obtained.

In order to determine how the HP strut heats up under normal operating conditions, a mileage test was carried out on a special version of a wheeled armoured personnel carrier. The tested vehicle was equipped with a suspension without a pressure compensation system. As part of the tests, the vehicle was driven over a distance of approximately 106 km at an average velocity of 20 km/h (limited by the terrain conditions) on a poor condition training ground road. The vehicle was fitted with all the equipment required for the tests. The ambient temperature during the tests was approximately 25°C. A pyrometer was used to measure the temperature of the outer

surface of the HP strut cylinders. Changes in vehicle height were measured on a horizontal flat surface using a photogrammetric method (the distance from the ground to a reference line on the vehicle hull were measured). The load of the of the road wheels were measured on a stationary overrun scale. In addition,

thermal images were taken with a thermal imaging camera. Measurements of the above quantities were taken before and immediately after the mileage test. The measurement results are summarised in Tab. 2.

Table 2. Measured suspension parameters before and after the mileage test.

| Axle | Temperature [°C] |                |             | Height [mm]    |                |            |                    | Normal force [daN] |                |             |                    |
|------|------------------|----------------|-------------|----------------|----------------|------------|--------------------|--------------------|----------------|-------------|--------------------|
|      | T <sub>o</sub>   | T <sub>k</sub> | ΔT          | h <sub>o</sub> | h <sub>k</sub> | Δh         | δ <sub>h</sub> [%] | N <sub>o</sub>     | N <sub>k</sub> | ΔN          | δ <sub>N</sub> [%] |
| 1    | 24.8             | 99.7           | <b>74.9</b> | 1480           | 1581           | <b>101</b> | 6.83               | 3300               | 3630           | <b>330</b>  | 10,0               |
| 2    | 25.3             | 64.3           | <b>39.0</b> | 1483           | 1592           | <b>109</b> | 7.36               | 3290               | 2930           | <b>-360</b> | -10,9              |
| 3    | 24.8             | 72.1           | <b>47.3</b> | 1487           | 1604           | <b>119</b> | 8.03               | 3420               | 3480           | <b>60</b>   | 1,75               |
| 4    | 24.6             | 77.8           | <b>53.2</b> | 1490           | 1615           | <b>125</b> | 8.42               | 3470               | 3380           | <b>-90</b>  | -2,59              |

Analysis of the results shows that the HP struts heat up unevenly, with the first axle suspension having the highest temperature (99.7°C). The wheels on the first axle are the first to encounter ground irregularities and are subjected to the highest loads. In addition, the deflection of their suspension is influenced by the angular vibrations of the vehicle's hull. The HP struts of the second axle reach the lowest temperature due to the unloading by the first axle. On the third and fourth axles, there were no significant differences in the temperature measured. There was also a change in the static deflection of the HP struts and consequently in the vehicle's ground clearance and height. This increased by 101 mm at the rear and by as much as 125 mm at the front. Fig. 10 shows a comparison of the vehicle height at the front.

The result of the uneven increase in the temperature of the HP struts, in the absence of a system to compensate for these changes, is an uneven change in the pressure of the operating media and therefore also in the vehicle pressure on the ground. The normal reactions from ground of the first axle wheels increased approximately about 10% compared to the reactions measured before the mileage test, while for the second axle it decreased approximately about 11%. The difference in reactions between the right wheels of the first and second axle wheels after the mileage test was approximately 7 kN. For the third and fourth axle wheels, the normal reaction do not change significantly, due to the similar temperature variation range of the HP struts. Both before and after the test, the difference in reactions on the wheels of these axles does not exceed 100 daN.

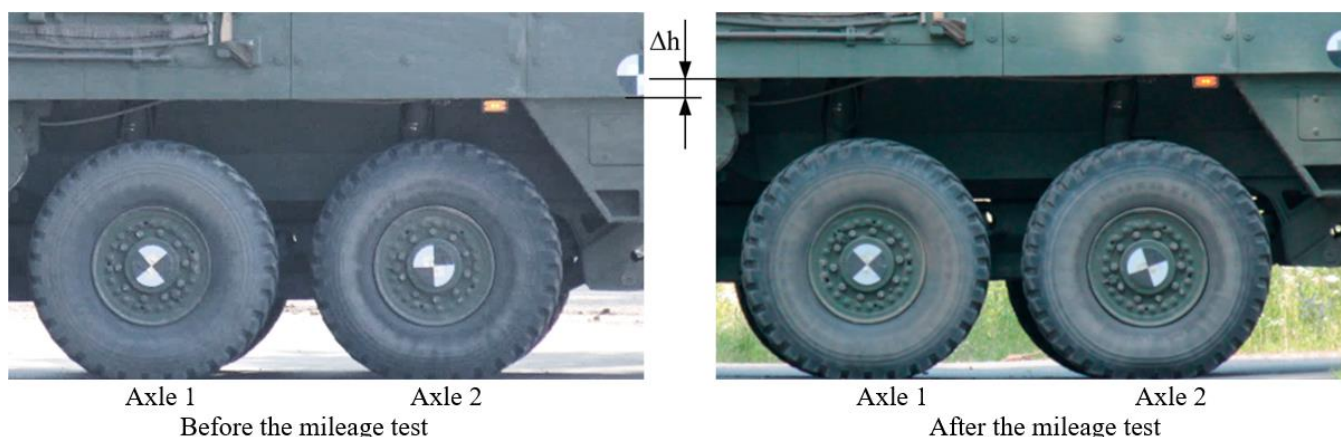


Fig. 10. Change in height of armoured personnel carrier before and after the mileage test.

Fig. 11 shows a thermographic image taken after the mileage test. It shows strong heating of the first axle strut (its upper part). Unfortunately, the main part of the cylinder (with the highest temperature) is hidden by the wheel with the tyre. It is therefore not possible to read the temperature values from this image. It

does, however, show which components other than the HP struts are subject to significant heating. This is important from the point of view of the vehicle's detectability in the thermal imaging cameras of the observation systems used in combat vehicles.



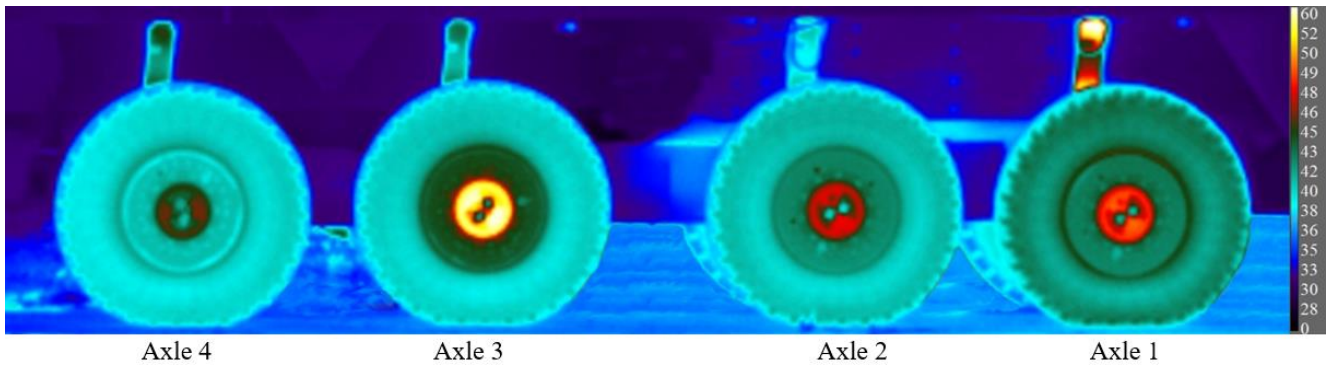


Fig. 11. Thermal image of the carrier running gear after the mileage test (temperature in °C).

## 5. Conclusions

HP suspension is increasingly being used in military vehicles because of their advantages. They provide a high level of ride smoothness and comfort. In addition, the vehicle's ground clearance can be adjusted by varying the initial pressure in the system.

Experimental results show that at low piston velocities, friction force is the main source of resistance in HP suspension. Its value increases with strut compression (increase in internal pressure).

The prepared model correctly reproduces the operation of a HP strut used in an armoured personnel carrier. Close agreement between simulation and experimental results was obtained assuming a polytropic gas process (for a polytropic exponent equal to 1.3). Unfortunately, its value is depending on the gas compression rate (the velocity of relative movement of the HP strut elements), as well as the pressure and temperature prevailing in the system. At higher velocities, its value will tend towards the exponent of the adiabatic process (which is equal to 1.4 for nitrogen under normal conditions). When the strut is fully compressed, the gas pressure increases to a value of

approximately 50 MPa and for this the adiabatic exponent should take a value greater than 1.4.

The value of the initial pressure in the gas chamber has a significant influence on the characteristics of a HP suspension. Increasing the pressure reduces the static deflection value (increasing vehicle ground clearance), while reducing the stiffness of the suspension. An increase in temperature increases the volume of oil and gas and, with the strut fully extended, also increases the initial pressure.

Under realistic operating conditions, changes in static deflection values also occur as a result of dynamic driving causing intense heating of the HP strut - especially the first axle. On multi-axle designs, this also leads to changes in the loads of the road wheels. Tests have shown a 10% increase in wheel reaction force on the first axle due to uneven heating of the strut. The solution to this problem is to use a system on the vehicle to compensate for the pressure variations.

Further work should include vibration energy dissipation mechanisms in the developed model. However, this requires determining the effect of pressure on the frictional forces in the seals and determining the damping characteristics over a wider range of velocities.

## Funding

This work was financed/co-financed by Military University of Technology under research project UGB 762/2022.

## References

1. Agarwal NK, Lawson CP. A practical method to account for seal friction in aircraft hydraulic actuator preliminary design. Proceedings of the Institution of Mechanical Engineers, Part G: Journal of Aerospace Engineering 2017; 231(5): 941-950, <https://doi.org/10.1177/0954410016645371>.
2. Bauer W. Hydropneumatic Suspension Systems, Springer-Verlag Berlin Heidelberg: 2011, ISBN 978-3-642-15146-0, <https://doi.org/10.1007/978-3-642-15147-7>.
3. Congbin Y, Xiaodong G, Zhifeng L, Ligang C, Qiang C, Caixia Z. Modeling and analysis of the vibration characteristics of a new type of in-arm hydropneumatic suspension of a tracked vehicle. Journal of Vibroengineering 2016; 18(7): 4627-4646,

<https://doi.org/10.21595/jve.2016.16800>.

4. Feng J, Matthews C, Zheng S, Yu F, Gao D. Hierarchical Control Strategy for Active Hydropneumatic Suspension Vehicles Based on Genetic Algorithms. *Advances in Mechanical Engineering* 2015; 7(2): 951050, <https://doi.org/10.1155/2014/951050>.
5. Han S, Chao Z, Liu X. Research on the Effects of Hydropneumatic Parameters on Tracked Vehicle Ride Safety Based on Cosimulation. *Shock and Vibration* 2017; Article ID 1256536: 1-10, <https://doi.org/10.1155/2017/1256536>.
6. Hryciów Z. An Investigation of the Influence of Temperature and Technical Condition on the Hydraulic Shock Absorber Characteristics. *Applied Sciences* 2022; 12(24): 12765, <https://doi.org/10.3390/app122412765>.
7. Hryciów Z, Małachowski J, Rybak P, Wiśniewski A. Research of Vibrations of an Armoured Personnel Carrier Hull with FE Implementation. *Materials* 2021; 14(22): 6807, <https://doi.org/10.3390/ma14226807>
8. Hryciów Z, Rybak P, Gieleta R. The influence of temperature on the damping characteristic of hydraulic shock absorbers. *Eksploatacja i Niezawodność – Maintenance and Reliability* 2021; 23 (2): 346–351, <http://doi.org/10.17531/ein.2021.2.14>.
9. Kinagi GV, Wadkar S, Sonawane D. Mathematical Modeling of Hydropneumatic Suspension System. *SAE Technical Paper Series* 2013; 2013-01-1928: 1-10, <https://doi.org/10.4271/2013-01-1928>.
10. Konieczny L, Burdzik R, Węgrzyn T. Analysis of Structural and Material Aspects of Selected Elements of a Hydropneumatic Suspension System in a Passenger Car. *Archives of Metallurgy and Materials* 2016; 61(1): 79-83, <https://doi.org/10.1515/amm-2016-0018>.
11. Lin D, Yang F, Gong D, Rakheja S. Design and experimental modeling of a compact hydro-pneumatic suspension strut. *Nonlinear Dynamics* 2020; 100(4): 3307–3320, <https://doi.org/10.1007/s11071-020-05714-3>
12. Oscarsson M. *A Hydropneumatic Suspension Parameter Study on Heavy Multi-axle Vehicle Handling*, Royal Institute of Technology, Sztokholm: 2015.
13. Pan Q, Zeng Y, Li Y, Jiang X, Huang M. Experimental investigation of friction behaviors for double-acting hydraulic actuators with different reciprocating seals. *Tribology International* 2021; 153 (106506): 1-14, <https://doi.org/10.1016/j.triboint.2020.106506>.
14. Qin B, Zeng R, Li X, Yang J. Design and Performance Analysis of the Hydropneumatic Suspension System for a Novel Road-Rail Vehicle. *Applied Sciences* 2021; 11(5): 1-16, <https://doi.org/10.3390/app11052221>.
15. Siminski P. Aspect of Simulation and Experimental Research Studies on Wheeled Armored Fighting Vehicles with Hydropneumatic Suspension. *SAE Technical Paper* 2010-01-0651, 2010. <https://doi.org/10.4271/2010-01-0651>
16. Sun H, Li R, Xu J, Xu F, Zhang B, Dong X. Fractional Modeling and Characteristic Analysis of Hydro-Pneumatic Suspension for Construction Vehicles. *Processes* 2021; 9(8): 1414, <https://doi.org/10.3390/pr9081414>.
17. Tran X, Khaing W, Endo H, Yanada H. Effect of friction model on simulation of hydraulic actuator. *Proceedings of the Institution of Mechanical Engineers, Part I: Journal of Systems and Control Engineering* 2014; 228(9) :690-698, <https://doi.org/10.1177/0959651814539476>.
18. van der Westhuizen SF, Els PS. Comparison of different gas models to calculate the spring force of a hydropneumatic suspension. *Journal of Terramechanics* 2015; 57: 41-59, <https://doi.org/10.1016/j.jterra.2014.11.002>.
19. Wu W, Tang H, Zhang S. High-Precision Dynamics Characteristic Modeling Method Research considering the Influence Factors of Hydropneumatic Suspension. *Shock and Vibration* 2020; Article ID 8886631: 1-21, <https://doi.org/10.1155/2020/8886631>.
20. Yin C, Zhai X, Sun X, Wang S, Wong PK. Design and performance research of a hydro-pneumatic suspension with variable damping and stiffness characteristics. *Journal of Mechanical Science and Technology* 2022; 36 (10): 4913-4923, <http://doi.org/10.1007/s12206-022-0905-0>.